Ratios of helicity amplitudes for exclusive ρ^0 electroproduction on transversely polarized proton

Serguei Manaenkov on behalf of the HERMES collaboration[1,⋆]

[1] *National Research Centre "Kurchatov Institute", Petersburg Nuclear Physics Institute, Russia*

Abstract. Exclusive ρ^0-meson electroproduction is studied by the HERMES experiment, using the 27.6 GeV longitudinally polarized electron/positron beam of HERA and a transversely polarized hydrogen target, in the kinematic region 1.0 GeV^2 < Q^2 < 7.0 GeV^2, 3.0 GeV < W < 6.3 GeV, and $-t'$ < 0.4 GeV^2. Using an unbinned maximum-likelihood method, 25 parameters are extracted. They determine the real and imaginary parts of the ratios of certain helicity amplitudes describing ρ^0-meson production by a virtual photon, where the denominator is the dominant amplitude $F_{0\frac{1}{2}0\frac{1}{2}}$. The latter is the nucleon-helicity-non-flip amplitude, which describes the production of a longitudinal ρ^0 meson by a longitudinal virtual photon. The transverse target polarization allows for the first time the extraction of ratios of a number of nucleon-helicity-flip amplitudes to $F_{0\frac{1}{2}0\frac{1}{2}}$. The ratios of nucleon-helicity-non-flip amplitudes are found to be in good agreement with those from the previous HERMES analysis.

1 Introduction

Exclusive electroproduction of vector mesons (V) on nucleons (N) gives information both on the reaction mechanisms and the nucleon structure [1]. Electroproduction at high energies can be considered to consist of three subprocesses: i) the incident lepton emits a virtual photon γ^*, which dissociates into a quark-antiquark pair; ii) this $q\bar{q}$ pair interacts strongly with the nucleon; iii) the observed vector meson is formed from the scattered $q\bar{q}$ pair. In Regge phenomenology, the interaction of the $q\bar{q}$ pair with the nucleon proceeds through the exchange of a pomeron or/and exchange of secondary reggeons. If the quantum numbers of the particle lying on the Regge trajectory are $J^P = 0^+,\ 1^-$, etc. (pomeron, ρ, f_2, ...), the process is denoted Natural Parity Exchange (NPE). Alternatively, the case of $J^P = 0^-,\ 1^+$, etc. (π, a_1, ...) corresponds to Unnatural Parity Exchange (UPE). In the framework of perturbative quantum chromodynamics valid at large photon virtuality Q^2 and high photon-nucleon center-of-mass (CM) energy W, the nucleon structure can also be studied through hard exclusive meson production, as the process amplitude contains Generalized Parton Distributions (GPDs) (see review [1]). However, the factorization property that permits to extract GPDs is rigorously proved only for the amplitudes $F_{0\frac{1}{2}0\pm\frac{1}{2}}$ of longitudinal vector meson production by longitudinal virtual photons [2]. In the Goloskokov-Kroll (GK) model (see [3] and references therein), the validity of factorization is assumed for some other amplitudes in addition to $F_{0\frac{1}{2}0\pm\frac{1}{2}}$ and this assumption is justified with a good description of the existing data. The presented HERMES data can be well described in the GK

⋆e-mail: manaenkov_si@pnpi.nrcki.ru

model if the pion exchange is taken into account (see [4] and references therein). This means that the GPD-based approach should be modified at intermediate energies and Q^2.

All observables in vector-meson electroproduction can be expressed in terms of the helicity amplitudes in the CM system describing ρ^0-meson production by a virtual photon. In particular, Spin-Density-Matrix Elements (SDMEs) are functions of the helicity amplitude ratios (HARs). Therefore HARs can be extracted from the data as was shown in [5]. For the first time, HARs with nucleon-helicity flip are obtained in the present analysis since the data on ρ^0-meson production by the longitudinally polarized electrons/positrons on a transversely polarized hydrogen target are accumulated.

2 Spin-density-matrix elements and helicity amplitudes

The SDMEs are the Fourier coefficients in angular distribution of the final-state particles. In the present paper, the formalism proposed in [6] for SDMEs is used. Any SDME can be expressed as a ratio of two sums of bilinear products of the helicity amplitudes $F_{\lambda_V \lambda'_N \lambda_\gamma \lambda_N}$ and their complex conjugate quantities $F^*_{\lambda_V \lambda'_N \lambda_\gamma \lambda_N}$. Here, $F_{\lambda_V \lambda'_N \lambda_\gamma \lambda_N}$ is the helicity amplitude of the process $\gamma^*(\lambda_\gamma) + N(\lambda_N) \rightarrow V(\lambda_V) + N(\lambda'_N)$, where the particle helicities are given in parentheses. The helicity amplitudes depend on W, Q^2, and $t' = t - t_{min}$, where t is the Mandelstam variable and $-t_{min}$ represents the smallest kinematically allowed value of $-t$ at fixed W and Q^2.

Any helicity amplitude can be decomposed into a sum of a NPE ($T_{\lambda_V \lambda'_N \lambda_\gamma \lambda_N}$) and an UPE ($U_{\lambda_V \lambda'_N \lambda_\gamma \lambda_N}$) amplitude: $F_{\lambda_V \lambda'_N \lambda_\gamma \lambda_N} = T_{\lambda_V \lambda'_N \lambda_\gamma \lambda_N} + U_{\lambda_V \lambda'_N \lambda_\gamma \lambda_N}$, for details see [6, 7]. The amplitudes obey the symmetry relations that hold because of parity conservation (see, e.g., [6, 7])

$$T_{\lambda_V \lambda'_N \lambda_\gamma \lambda_N} = (-1)^{-\lambda_V + \lambda_\gamma} T_{-\lambda_V \lambda'_N - \lambda_\gamma \lambda_N} = (-1)^{-\lambda_N + \lambda'_N} T_{\lambda_V - \lambda'_N \lambda_\gamma - \lambda_N}, \quad (1)$$

$$U_{\lambda_V \lambda'_N \lambda_\gamma \lambda_N} = -(-1)^{-\lambda_V + \lambda_\gamma} U_{-\lambda_V \lambda'_N - \lambda_\gamma \lambda_N} = -(-1)^{-\lambda_N + \lambda'_N} U_{\lambda_V - \lambda'_N \lambda_\gamma - \lambda_N}. \quad (2)$$

These symmetry properties of the helicity amplitudes permit to introduce the abbreviated notations:

$$T^{(1)}_{\lambda_V \lambda_\gamma} \equiv T_{\lambda_V \frac{1}{2} \lambda_\gamma \frac{1}{2}}, \;\; U^{(1)}_{\lambda_V \lambda_\gamma} \equiv U_{\lambda_V \frac{1}{2} \lambda_\gamma \frac{1}{2}}, \;\; T^{(2)}_{\lambda_V \lambda_\gamma} \equiv T_{\lambda_V \frac{1}{2} \lambda_\gamma - \frac{1}{2}}, \;\; U^{(2)}_{\lambda_V \lambda_\gamma} \equiv U_{\lambda_V \frac{1}{2} \lambda_\gamma - \frac{1}{2}}. \quad (3)$$

All other amplitudes can be obtained from the symmetry relations given by (1 − 2). The HARs extracted in the present analysis are defined for $n = 1,\ 2$ as $t^{(n)}_{\lambda_V \lambda_\gamma} = T^{(n)}_{\lambda_V \lambda_\gamma} / T^{(1)}_{00}$, $u^{(n)}_{\lambda_V \lambda_\gamma} = U^{(n)}_{\lambda_V \lambda_\gamma} / T^{(1)}_{00}$.

3 Experiment and data analysis

3.1 Experiment

The data were accumulated with the HERMES spectrometer using the 27.6 GeV longitudinally polarized electron or positron beam of HERA and a gaseous hydrogen target. The HERMES setup included a forward spectrometer described in [8], in which the scattered lepton and the produced hadrons were detected within an angular acceptance of ±170 mrad horizontally and ±(40−140) mrad vertically. The tracking system had a momentum resolution of about 1.5% and an angular resolution of about 1 mrad. Lepton identification was accomplished using a transition-radiation detector, a preshower scintillator counter, and an electromagnetic calorimeter. The particle-identification system included also a dual-radiator ring-imaging Cherenkov detector [9] to identify hadrons. Combining the responses of the detectors in a likelihood method leads to an average lepton-identification efficiency of 98%, with a hadron contamination of less than 1%. The helicity of the beam was typically reversed every two months. The beam polarization was continuously measured by two Compton polarimeters [10, 11]. The average value of the beam polarization for the events used in the analysis is ±0.30 with a 0.03 uncertainty. A small part of the data were collected with an unpolarized target and the main part with a transversely polarized target [12], for which the polarization direction was reversed every 60 s to 180 s. The measured mean value of the target polarization is $\langle |P_T| \rangle = 0.72 \pm 0.06$ [13].

3.2 Data analysis

The ρ^0 mesons are produced and decay in the following exclusive reactions: $e + p \rightarrow e + p + \rho^0$, and $\rho^0 \rightarrow \pi^+ + \pi^-$. The event sample used in this analysis is practically the same as that used in [13]. The most important improvement is the application of a new tracking algorithm, which is based on a Kalman filter [14]. For the present analysis, the data are required to fulfill the following criteria: i) The scattered lepton has to have an energy larger than 3.5 GeV in order to not introduce effects from varying trigger thresholds. ii) The longitudinal beam polarization is restricted to the interval $15\% < |P_B| < 80\%$. iii) Events with exactly two oppositely charged hadrons and one lepton with the same charge as the beam lepton are selected. All tracks are required to originate from the same vertex. iv) No calorimeter clusters were observed (no π^0 is detected). v) The two-pion invariant mass is required to obey 0.6 GeV$\leq$ M($\pi^+\pi^-$)$\leq$ 1.0 GeV. vi) The recoiling proton was not detected, but instead reconstructed through the missing energy. Taking into account the spectrometer resolution, the missing energy ΔE has to lie in the interval -1.0 GeV $< \Delta E <$ 0.8 GeV. Here, $\Delta E = \frac{M_X^2 - M_p^2}{2M_p}$, with M_p being the proton mass and $M_X^2 = (p + q - p_{\pi^+} - p_{\pi^-})^2$ the missing mass squared, where p, q, p_{π^+}, and p_{π^-} are the four-momenta of target nucleon, virtual photon, and each of the two pions respectively. The distribution of missing energy ΔE, shown in [13], exhibits a clearly visible exclusive peak. vii) The kinematic constraints $Q^2 > 1.0$ GeV^2, 6.3 GeV $> W >$ 3 GeV, $-t' < 0.4$ GeV^2 are applied.

After application of all these requirements, the data sample contains 8741 events. These data are referred to in the following as data in the "entire kinematic region". The applied constraints do not fully suppress the background contribution. The exclusive sample contains contributions from double-diffractive processes, which should be negligible in the low ΔE region, from non-resonant $\pi^+\pi^-$ pair production, which is of the order of $1 - 2\%$ [13], from Δ-isobar excitation, which contribution in the HERMES acceptance is less than 7% [15] and from semi-inclusive deep-inelastic scattering (SIDIS) events. The presented results are not corrected for the former three processes, while a correction is applied for SIDIS background. The shaded histogram of missing energy ΔE (presented in [13]) shows SIDIS background obtained from a PYTHIA Monte Carlo (MC) simulation. It is normalized to the data in the region of 2 GeV $< \Delta E <$ 20 GeV. The simulation is used to determine the fraction of SIDIS background under the exclusive peak. This fraction f_{bg} increases from 7% to 23% for increasing $-t'$ and amounts on average to 11%. A fit of the angular distribution of the SIDIS MC events under the exclusive peak is performed. The obtained function W_{bg} having no free parameters and the angular distribution W_ρ of the exclusive ρ^0 production are combined to give the total angular distribution $W_{tot} = (1-f_{bg})W_\rho + f_{bg}W_{bg}$. The function W_{tot} is used in an unbinned maximum-likelihood method, the detector properties are taken into account with using MC simulation. The contribution of background from SIDIS events to the obtained amplitude ratios is considered as one of the main sources of systematic uncertainty. This uncertainty is calculated as difference between HARs obtained for $f_{bg} = 0$ and HARs extracted when the background corrections are taken into account.

4 Results

The HARs obtained from the 25-parameter fit in the entire kinematic region ($\langle W \rangle = 4.73$ GeV, $\langle Q^2 \rangle = 1.93$ GeV^2, $\langle -t' \rangle = 0.132$ GeV^2) are shown in figure 1. While the phase of $u_{11}^{(1)}$ is fixed according to the results of [16, 17], its modulus is fit so that the two crosses represent the results of fitting one free parameter. The value of Im[$t_{11}^{(1)}$] (open square) represents the result of [5]; its error bar shows the total uncertainty. The shadowed area corresponds to results obtained here, but also obtained in [5], while all other points are calculated for the first time. As is seen from figure 1, all HARs except $t_{11}^{(1)}$, $t_{01}^{(1)}$, and $u_{11}^{(1)}$, are compatible with zero within their total uncertainties. The HAR $t_{01}^{(1)}$ is responsible for the

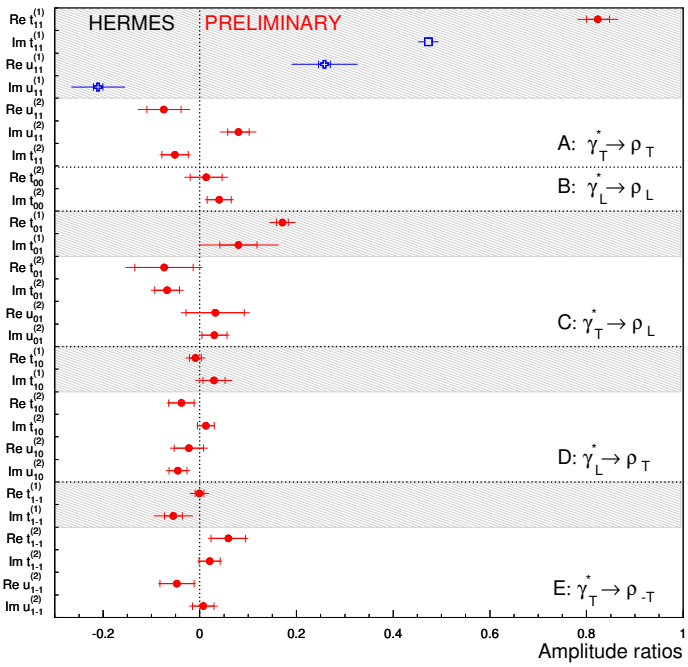

Figure 1. Helicity-amplitude ratios in the entire kinematic region. The phase of $u^{(1)}_{11}$ (open crosses) is fixed according to the results of [16, 17], its modulus is fit. The value of $\mathrm{Im}[t^{(1)}_{11}]$ (open square) represents the result of [5]; its error bar shows the total uncertainty. For all other points the inner error bars represent the statistical uncertainty, while the outer ones represent statistical and systematic uncertainties added in quadrature.

violation of the s-channel helicity conservation approximation, while $u^{(1)}_{11}$ shows the role of UPE in ρ^0-meson production. Note that even the HARs compatible with zero are informative and can be used to fix parameters of theoretical models (see, e.g., the paper by S.V. Goloskokov in these proceedings).

A comparison of the SDMEs directly obtained from the HERMES data in [7] and [13] to those calculated with the HARs extracted in the present analysis is shown in figures 2-4. The correlation matrix for the 25 parameters is taken into account for the calculation of the statistical uncertainties of the SDMEs in the Diehl representation [6] $u^{\lambda_V\lambda'_V}_{\lambda_\gamma\lambda'_\gamma}$, $n^{\lambda_V\lambda'_V}_{\lambda_\gamma\lambda'_\gamma}$, and $s^{\lambda_V\lambda'_V}_{\lambda_\gamma\lambda'_\gamma}$ obtained from the HARs. The SDMEs $n^{\lambda_V\lambda'_V}_{\lambda_\gamma\lambda'_\gamma}$ and $s^{\lambda_V\lambda'_V}_{\lambda_\gamma\lambda'_\gamma}$, presented in figures 3 and 4, have linear contributions of the small HARs $t^{(2)}_{\lambda_V\lambda_\gamma}$ and $u^{(2)}_{\lambda_V\lambda_\gamma}$, respectively. These SDMEs can only be extracted from measurements with a transversely polarized target so that the nucleon-helicity-flip amplitude ratios $t^{(2)}_{\lambda_V\lambda_\gamma}$ and $u^{(2)}_{\lambda_V\lambda_\gamma}$ are extracted in this paper for the first time. The total uncertainty is the sum in quadrature of the statistical and the total systematic uncertainties. The SDMEs in figures 3-4 are reordered according to the SDME classes proposed in [7, 13]. Those SDMEs that can be extracted only from data taken with a longitudinally polarized lepton beam are shown in shaded areas.

Figure 2 shows that for each SDME $u^{\lambda_V\lambda'_V}_{\lambda_\gamma\lambda'_\gamma}$ determined from our present results for HARs, there exists an SDME $u^{\lambda_V\lambda'_V}_{\lambda_\gamma\lambda'_\gamma}$ published in [7]. However, figures 3 and 4 show that for some of the calculated SDMEs $n^{\lambda_V\lambda'_V}_{\lambda_\gamma\lambda'_\gamma}$ and $s^{\lambda_V\lambda'_V}_{\lambda_\gamma\lambda'_\gamma}$ no published results from [13] exist, because the beam polarization was not exploited in the analysis performed in [13]. While in [7] and [13] a total of 53 SDMEs could be extracted, the amplitude method presented here allows for the calculation of 71 SDMEs based on the

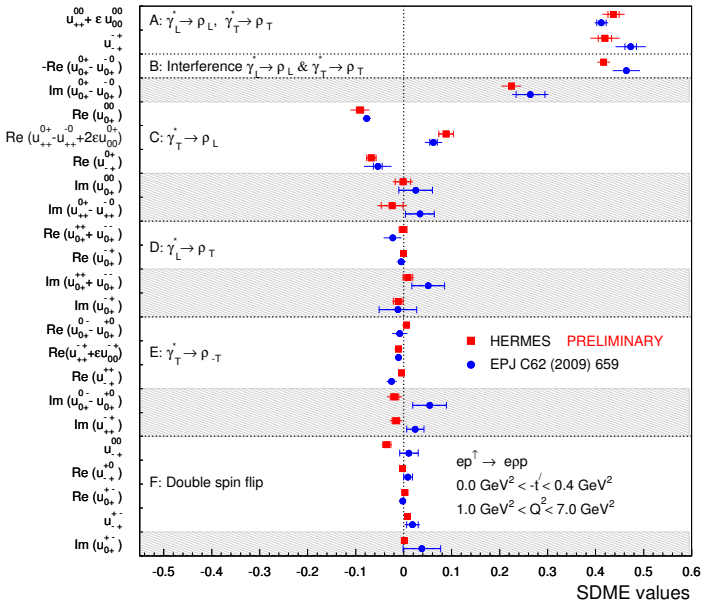

Figure 2. Comparison of the Diehl SDMEs [6] $u^{\lambda_V \lambda'_V}_{\lambda_\gamma \lambda'_\gamma}$ calculated from the helicity-amplitude ratios (red squares) and the SDMEs (blue circles) directly extracted in [7] in the entire kinematic region. For the first case, a 25-parameter fit is used. The points in the shaded area show SDMEs that can be obtained only if the beam is longitudinally polarized. The inner (outer) error bars represent the statistical (total) uncertainty.

extraction of 25 parameters. As seen from the figures, there is reasonable agreement between SDMEs directly extracted in [7, 13] and those calculated from the HARs.

References

[1] M. Diehl, Phys. Rep. **388**, 41 (2003)
[2] J.C. Collins, L. Frankfurt, M.S. Strikman, Phys. Rev. D **56**, 2982 (1997)
[3] S.V. Goloskokov and P. Kroll, Eur. Phys. J. C **53**, 367 (2008)
[4] S.V. Goloskokov and P. Kroll, Eur. Phys. J. A **50**, 146 (2014)
[5] A. Airapetian et al. (HERMES Collaboration), Eur. Phys. J. C **71**, 1609 (2011)
[6] M. Diehl, JHEP **0709**, 064 (2007)
[7] A. Airapetian et al. (HERMES Collaboration), Eur. Phys. J. C **62**, 659 (2009)
[8] K. Ackerstaff et al. (HERMES Collaboration), Nucl. Instr. and Meth. A **417**, 230 (1998)
[9] N. Akopov et al. (HERMES Collaboration), Nucl. Instr. and Meth. A **479**, 511 (2002)
[10] D.P. Barber et al. (HERMES Collaboration), Nucl. Instr. and Meth. A **329**, 79 (1993)
[11] M. Beckmann et al. (HERMES Collaboration), Nucl. Instr. and Meth. A **479**, 334 (2002)
[12] A. Airapetian et al. (HERMES Collaboration), Nucl. Instr. and Meth. A **540**, 68 (2005)
[13] A. Airapetian et al. (HERMES Collaboration), Phys. Lett. B **679**, 100 (2009)
[14] R. Fruhwirth, Nucl. Instr. and Meth. A **262**, 444 (1987)
[15] M. Tytgat, DESY-THESIS-2001-014 (2001)
[16] A. Airapetian et al. (HERMES Collaboration), Phys. Lett. B **513**, 301 (2001)
[17] A. Airapetian et al. (HERMES Collaboration), Eur. Phys. J. C **29**, 171 (2003)

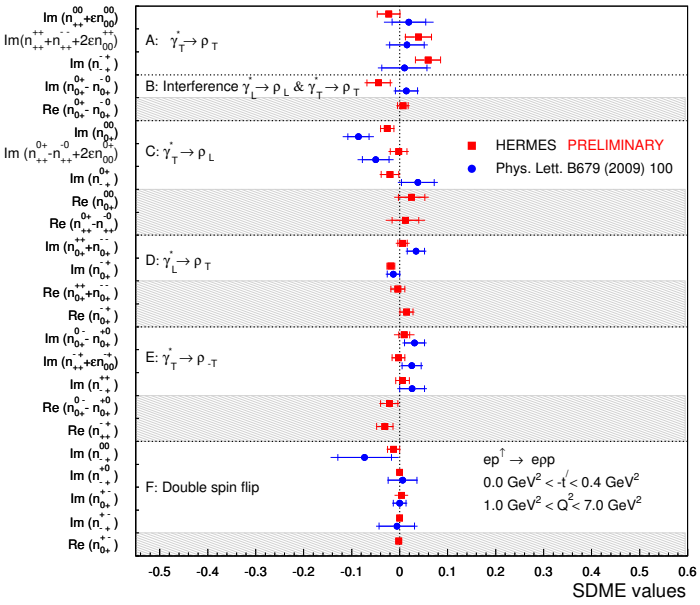

Figure 3. Comparison of the Diehl SDMEs [6] $n^{\lambda_V \lambda'_V}_{\lambda_\gamma \lambda'_\gamma}$ calculated from the helicity-amplitude ratios (red squares) and the SDMEs (blue circles) directly extracted in [13] in the entire kinematic region. For the first case, a 25-parameter fit is used. The points in the shaded area show SDMEs that can be obtained only if the beam is longitudinally polarized. The inner (outer) error bars represent the statistical (total) uncertainty.

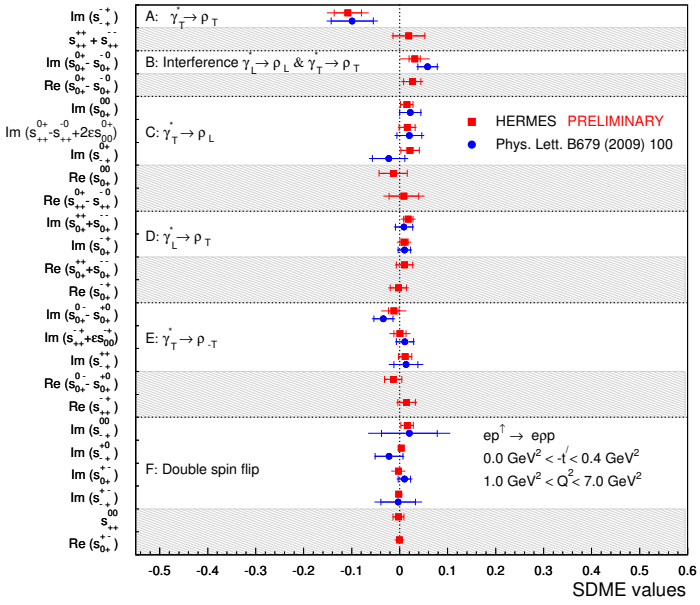

Figure 4. Comparison of the Diehl SDMEs [6] $s^{\lambda_V \lambda'_V}_{\lambda_\gamma \lambda'_\gamma}$ calculated from the helicity-amplitude ratios (red squares) and the SDMEs (blue circles) directly extracted in [13] in the entire kinematic region. For the first case, a 25-parameter fit is used. The points in the shaded area show SDMEs that can be obtained only if the beam is longitudinally polarized. The inner (outer) error bars represent the statistical (total) uncertainty.